Cell Death and Differentiation (2008) 15, 751–761

www.nature.com/cdd

Structural and functional analysis of the interaction between the agonistic monoclonal antibody Apomab and the proapoptotic receptor DR5

C Adams[1], K Totpal[2], D Lawrence[3], S Marsters[3], R Pitti[3], S Yee[2], S Ross[2], L Deforge[4], H Koeppen[5], M Sagolla[5], D Compaan[6], H Lowman[1], S Hymowitz[6] and A Ashkenazi*[,3]

Activation of the proapoptotic receptor death receptor5 (DR5) in various cancer cells triggers programmed cell death through the extrinsic pathway. We have generated a fully human monoclonal antibody (Apomab) that induces tumor cell apoptosis through DR5 and investigated the structural features of its interaction with DR5. Biochemical studies showed that Apomab binds DR5 tightly and selectively. X-ray crystallographic analysis of the complex between the Apomab Fab fragment and the DR5 ectodomain revealed an interaction epitope that partially overlaps with both regions of the Apo2 ligand/tumor necrosis factor-related apoptosis-inducing ligand binding site. Apomab induced DR5 clustering at the cell surface and stimulated a death-inducing signaling complex containing the adaptor molecule Fas-associated death domain and the apoptosis-initiating protease caspase-8. Fc crosslinking further augmented Apomab's proapoptotic activity. *In vitro*, Apomab triggered apoptosis in cancer cells, while sparing normal hepatocytes even upon anti-Fc crosslinking. *In vivo*, Apomab exerted potent antitumor activity as a single agent or in combination with chemotherapy in xenograft models, including those based on colorectal, non-small cell lung and pancreatic cancer cell lines. These results provide structural and functional insight into the interaction of Apomab with DR5 and support further investigation of this antibody for cancer therapy.
Cell Death and Differentiation (2008) **15,** 751–761; doi:10.1038/sj.cdd.4402306; published online 25 January 2008

Cancer is the second leading cause of death in the United States, with solid tumors accounting for most of the associated mortality.[1] Recent medical advances have improved cancer therapy, for example, by targeting growth-factor signaling pathways in malignant cells within tumors or in endothelial cells within the vessels that supply tumors with blood.[2] However, the need for therapies that can eradicate tumors remains largely unmet. A novel experimental approach, currently in clinical investigation, aims to trigger apoptosis (programmed cell death) in cancer cells by targeting proapoptotic death receptors (DRs).[3–6] Metazoan organisms use apoptosis as a homeostatic mechanism to eliminate cells of their own that are no longer needed or have become irreparably damaged.[7] In cancer, oncogene activation and genotoxic damage drive apoptosis; however, frequent inactivation of the p53 tumor suppressor – a crucial conduit between certain types of cellular damage and apoptosis – often enables tumor cells to escape apoptotic death.[8,9]

Apoptosis is carried out by specialized proteases called caspases, which function in cascade mode: first, initiator caspases (e.g. caspase-8, -9, and -10) are activated. In turn, these initiators cleave and activate effector caspases (e.g. caspase-3, -6 and -7), which drive the apoptotic cell death program.[10,11] Two principal signaling pathways control cellular caspase activation: the intrinsic pathway is initiated inside the cell in response to developmental cues or various types of cell stress, by specific members of the Bcl-2 gene family.[12–14] The proapoptotic Bcl-2 family members Bax and Bak lead to permeabilization of the mitochondrial outer membrane, and consequently, the release of specific factors that promote caspase activation in the cytosol. Key among these factors are cytochrome *c*, which cooperates with the adaptor Apaf-1 to activate initiator caspase-9, and Smac/Diablo, which antagonizes blockade of caspase-9 and of effector caspases by inhibitor of apoptosis proteins.[15] Taken together, these post-mitochondrial events trigger effector caspase activation and apoptotic cell death. The p53 tumor suppressor protein plays an important role in stimulating the intrinsic pathway in response to certain types of cellular stress, including DNA and microtubule damage.[9] Many conventional chemotherapeutic agents and radiotherapy exert antitumor activity by causing these latter types of cell damage. Tumor cells often can evade apoptosis activation in response to such treatments, because of inactivating mutations

[1]Department of Antibody Engineering, Genentech Inc., South San Francisco, CA, USA; [2]Department of Translational Oncology, Genentech Inc., South San Francisco, CA, USA; [3]Department of Molecular Oncology, Genentech Inc., South San Francisco, CA, USA; [4]Department of Assay and Automation Technology, Genentech Inc., South San Francisco, CA, USA; [5]Department of Research Pathology, Genentech Inc., South San Francisco, CA, USA and [6]Department of Protein Engineering, Genentech Inc., South San Francisco, CA, USA

*Corresponding author: A Ashkenazi, Department of Molecular Oncology, Genentech Inc., 1 DNA Way, MS 42, South San Francisco, CA 94080-4918, USA. Tel: 650 225 1853; Fax: 650 467 8195; E-mail: aa@gene.com

Keywords: Apo2L/TRAIL; death receptor; caspase; cancer

Abbreviations: Apo2L/TRAIL, Apo2 ligand/TNF-related apoptosis-inducing ligand; CRD, cysteine-rich domain; CDR, complementarity determining region; DISC, death-inducing signaling complex; DR, death receptor; ECD, extracellular domain; FADD, Fas-associated death domain; NSCLC, non-small cell lung cancer; PARA, proapoptotic receptor agonist

Received 08.10.07; revised 06.12.07; accepted 06.12.07; Edited by G Melino; published online 25.1.08

in the p53 gene, which occur in more than half of human cancers. Hence, there is a need for novel therapies that can help overcome this apoptosis resistance.

A second key signaling mechanism that controls caspase activation is the extrinsic pathway. This pathway is activated from outside the cell by specialized proapoptotic ligands that belong to the tumor necrosis factor (TNF) superfamily, such as Fas ligand (FasL) and Apo2 ligand/TNF-related apoptosis-inducing ligand (Apo2L/TRAIL).[3,16–18] These ligands have been found to interact with proapoptotic receptors on the surface of a target cell, leading to both receptor clustering and recruitment of an adaptor molecule called Fas-associated death domain (FADD). In turn, FADD recruits the apoptosis-initiating protease caspase-8 into a death-inducing signaling complex (DISC). The DISC activates caspase-8, leading to self-processing that releases active caspase molecules into the cytoplasm, where they can activate the effector caspases. In some cell types, the extrinsic pathway is amplified by cross-talk with the intrinsic pathway: caspase-8 cleaves and consequently activates the Bcl-2 family member Bid, which engages the intrinsic pathway through Bax and Bak.[7,18–20]

Because of its distinct, p53-independent mode of apoptosis activation, the extrinsic pathway provides an attractive target for potential cancer therapy. Of the proapoptotic receptors, the Apo2L/TRAIL receptors DR4 and DR5 are of particular interest because experimental studies have revealed that activation of these receptors can trigger apoptosis in various types of cancer cells, while sparing most normal cell types.[17,20] Two molecular types of proapoptotic receptor agonists (PARAs) that target DR4 and/or DR5, which have been described in the literature, are recombinant human Apo2L/TRAIL (rhApo2L/TRAIL), which stimulates both receptors,[21–23] and agonistic antibodies that activate either DR4 or DR5.[24–32] Efficacy of rhApo2L/TRAIL in preclinical cancer models has been documented, demonstrating compelling antitumor activity both as monotherapy and in combination with chemotherapy.[3,23] Here, we describe Apomab, a DR5 agonist antibody, determine the structure of its Fab fragment in complex with DR5 and characterize its antitumor activity *in vitro* and *in vivo*.

Results

Binding of Apomab to DR5. We used the phage display approach to develop a fully human, affinity-matured IgG1/λ3 monoclonal antibody (called Apomab) that triggers apoptosis upon interaction with human DR5. We characterized the binding selectivity of Apomab by comparing its interaction with the extracellular domain (ECD) of all the known human Apo2L/TRAIL receptors, namely, DR4, DR5, decoy receptor (DcR) 1, DcR2 and OPG (expressed and purified as Fc fusion proteins). Apomab bound to DR5, but showed no detectable binding to any of the other receptors (Figure 1a). Competitive binding analysis indicated consistency between three independent Apomab preparations, with a half-maximal binding at 212 ± 15 ng/ml (1.4 ± 0.1 nM) (Figure 1b). Using saturation analysis for the binding of ^{125}I-labeled Apomab to DR5-Fc, we measured an equilibrium dissociation constant (K_D) of 0.92 ± 0.01 nM (Figure 1c), in agreement with the competition data. Apomab bound with similar selectivity

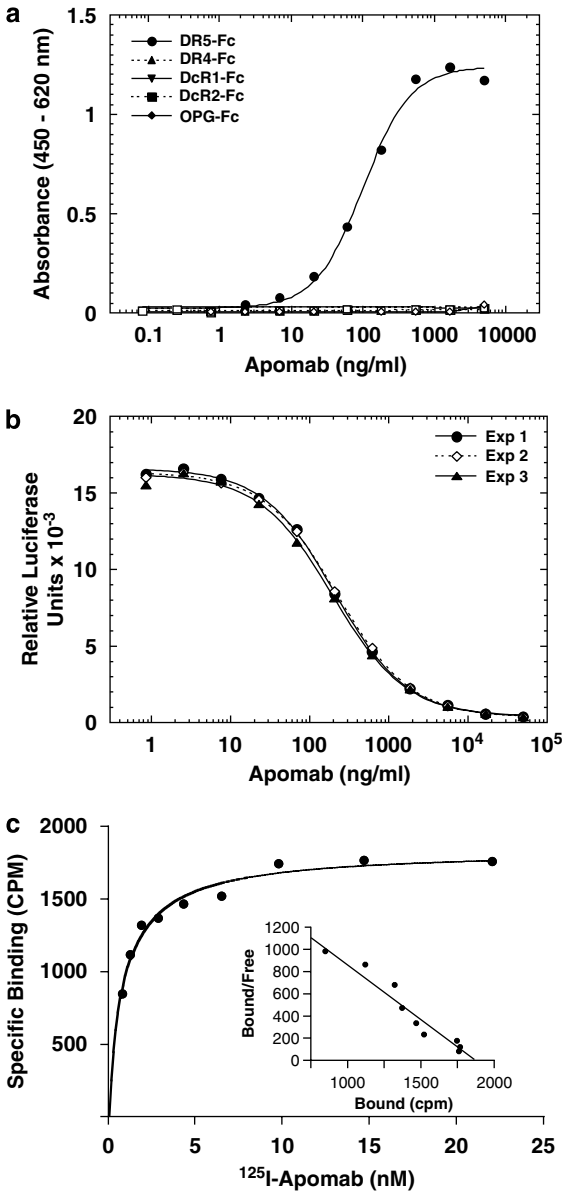

Figure 1 Binding of Apomab to DR5. (**a**) Apomab binding to purified human IgG1 Fc fusion proteins based on the human Apo2L/TRAIL receptors DR5, DR4, DcR1, DcR2 and OPG (Genentech Inc.). Binding was determined in ELISA format: each receptor–Fc fusion was coated onto microtiter wells and incubated with a serial dilution of Apomab for 2 h at room temperature. Bound Apomab was then detected using a horseradish peroxidase-conjugated goat F(ab′)$_2$ anti-human IgG antibody. (**b**) Competitive binding assay comparing DR5 binding of three independent preparations of Apomab. Binding was measured using an electrochemiluminescent (ECL) solution-phase assay. Human DR5-Fc was biotinylated and Apomab was conjugated to a ruthenium chelate. Fixed concentrations of biotin-DR5-Fc and labeled Apomab were incubated with a dilution series of unlabeled Apomab for 2 h at room temperature. Streptavidin magnetic beads were then added for 30 min and the plates were read in an ECL signal analyzer to detect the complexes of biotin-DR5-Fc and labeled Apomab. (**c**) Saturation analysis. Apomab was labeled with ^{125}I and incubated at the indicated concentrations with DR5-Fc-coated on microtiter wells for 1 h at room temperature. Nonspecific binding was determined in the presence of excess unlabeled Apomab. A nonlinear one-site curve fit indicated a K_D of 0.92 ± 0.01 nM

to the cynomolgus monkey Apo2L/TRAIL receptors (Supplementary Figure 1).

Crystallographic analysis of the Apomab–DR5 complex. To determine how Apomab binds to DR5 at the atomic level, we crystallized the complex between the Fab fragment of Apomab and the extracellular region of human DR5. We obtained a crystal structure at 3.2-Å resolution (Figure 2a; Supplementary Figures 2 and 3; and Supplementary Table 1). The solved structure showed that Apomab binds to DR5 at the junction between cysteine-rich domain (CRD) 2 and CRD3. The interface covers an area of approximately 1800 Å^2, split evenly between DR5 (~960 Å^2) and Apomab (840 Å^2). The interaction involves residues from the Apomab light-chain complementarity determining region (CDR) L1, L2 and L3 as well as heavy-chain CDRs H1, H2 and H3, with H3 contributing more residues and more surface area than any other CDRs. Figure 2b and Supplementary Figures 2c and 3 depict the previously published structure of Apo2L/TRAIL in complex with DR5[33] compared with the newly determined structure of the Apomab–DR5 complex. The Apomab-binding site on DR5 uses some of the same residues as those involved in contacting Apo2L/TRAIL, although the overlap between the two sites is not complete. Apo2L/TRAIL contacts two discrete DR5 regions: the first disulfide-bonded loop (the so-called A1 module) in CRD2 (residues 50–65) and in CRD3 (residues 90–111). The interaction between Apo2L/TRAIL and CRD3 is centered on DR5 residues 98–99, contacted by Gln 205 from the ligand. Mutation of Gln 205 has a negative effect on Apo2L/TRAIL bioactivity and results in impaired binding affinity for DR5 as well as DR4.[34] The Apomab–DR5 interface is centered in a nearly continuous region of DR5, comprising residues 62–90, with additional contributions from residues 99–105. DR5 residues Arg 65, Ser 68 and Lys 102 all cover greater than 100 Å^2 upon binding Apomab (Supplementary Figure 2a and b). In contrast to Apomab, another phage-derived DR5 antibody (BDF1), which we have characterized as having little or no agonistic activity, interacts with CRD2 but not CRD3 (Supplementary Figure 2c). In independent structures of DR5 bound to Apo2L/TRAIL or the Fab fragment of Apomab or BDF1, CRD1 and 2 show little change, yet CRD3 shows significant conformational diversity, suggesting that the orientation of this region is influenced by the binding epitope and may be important for DR5 activation (Supplementary Figure 4).

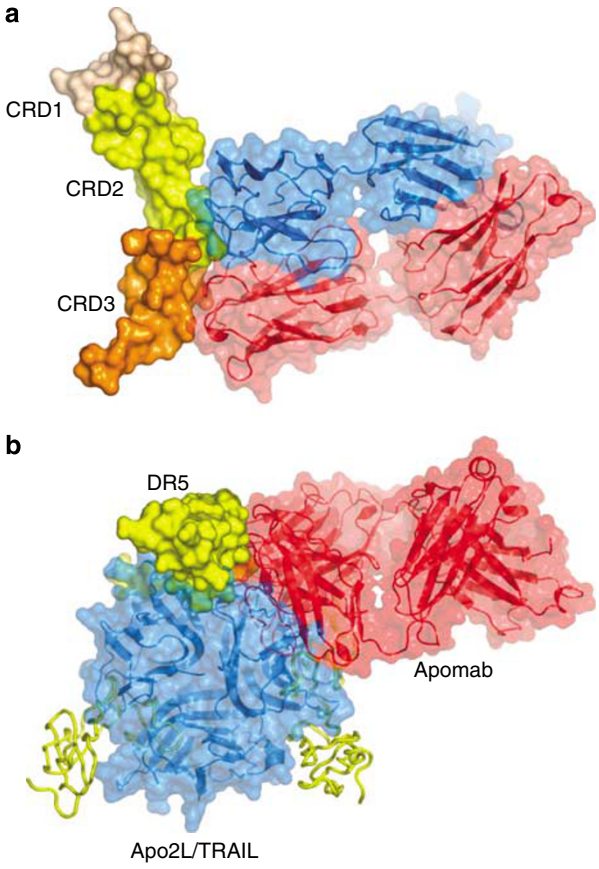

Figure 2 Structure of the Apomab Fab fragment in complex with the DR5 ectodomain. The Apomab–DR5 complex was generated by incubating purified Apomab Fab with an excess of purified human DR5-ECD protein, followed by purification over a Superdex-200 sizing column. The complex-containing fractions were pooled, concentrated and used for crystallization. The structure was solved (resolution: 3.2-Å) in space group P6 by molecular replacement with the program AMoRe using the structure 8FAB as a search model. (**a**) Apomab binds at the junction between CRD2 and CRD3. DR5 (brown, yellow and orange) and the Apomab Fab (light chain blue, heavy chain red) are shown as molecular surfaces. (**b**) Apo2L/TRAIL (blue) and Apomab (red) bind to overlapping yet distinct sites on DR5 (yellow). The structure of the Apomab Fab–DR5 complex is overlaid on the previously solved Apo2L/TRAIL–DR5 complex. For clarity, only one copy of DR5 is shown. Additional copies of DR5 that would bind at the Apo2L/TRAIL monomer–monomer interfaces are shown as yellow backbone ribbons

Proapoptotic activity of Apomab. Immunofluorescence staining of DR5 on H460 non-small cell lung cancer (NSCLC) cells indicated a dotted appearance in the plasma membrane (visualized by staining with cholera toxin subunit B) (Figure 3a). Stimulation with Apomab led to apparent clustering of DR5 at 15 min, followed by internalization at 30 and 60 min (Figure 3a and Supplementary Figure 5), similar to earlier data for Apo2L/TRAIL.[35] To examine the activation of DR5 at the biochemical level, we analyzed the ability of Apomab to induce a DR5-associated DISC. Immunoprecipitation of DR5 from Apomab-treated COLO205 colorectal cancer cells and H2122 NSCLC cells followed by immunoblot analysis indicated that Apomab induced recruitment of FADD and caspase-8 to DR5 and processing of caspase-8 within 15–60 min (Figure 3b). Accordingly, Apomab also induced processing of caspase-8 as detected in cell lysates (Figure 3d). H2122 cells showed more robust DISC activation by Apomab alone than did COLO205 cells; however, both cell lines were killed similarly well (see below), suggesting that the detectable difference in the DISC was not significantly consequential. Addition of an anti-Fc crosslinking antibody to Apomab further augmented DISC assembly and caspase-8 activation, consistent with the hypothesis that further receptor aggregation may enhance proapoptotic signaling (Figure 3). Comparable results were obtained with rhApo2L/TRAIL (Figure 3c and d), indicating that DR5 stimulation by Apomab suffices to trigger an apoptotic response in these cells. Similarly, Apomab and rhApo2L/TRAIL stimulated DISC assembly and caspase-8 activation in H460 cells (Supplementary Figure 6a and b).

Apomab induced a significant, dose-dependent loss of viability in COLO205 cells (Figure 4a) and activation

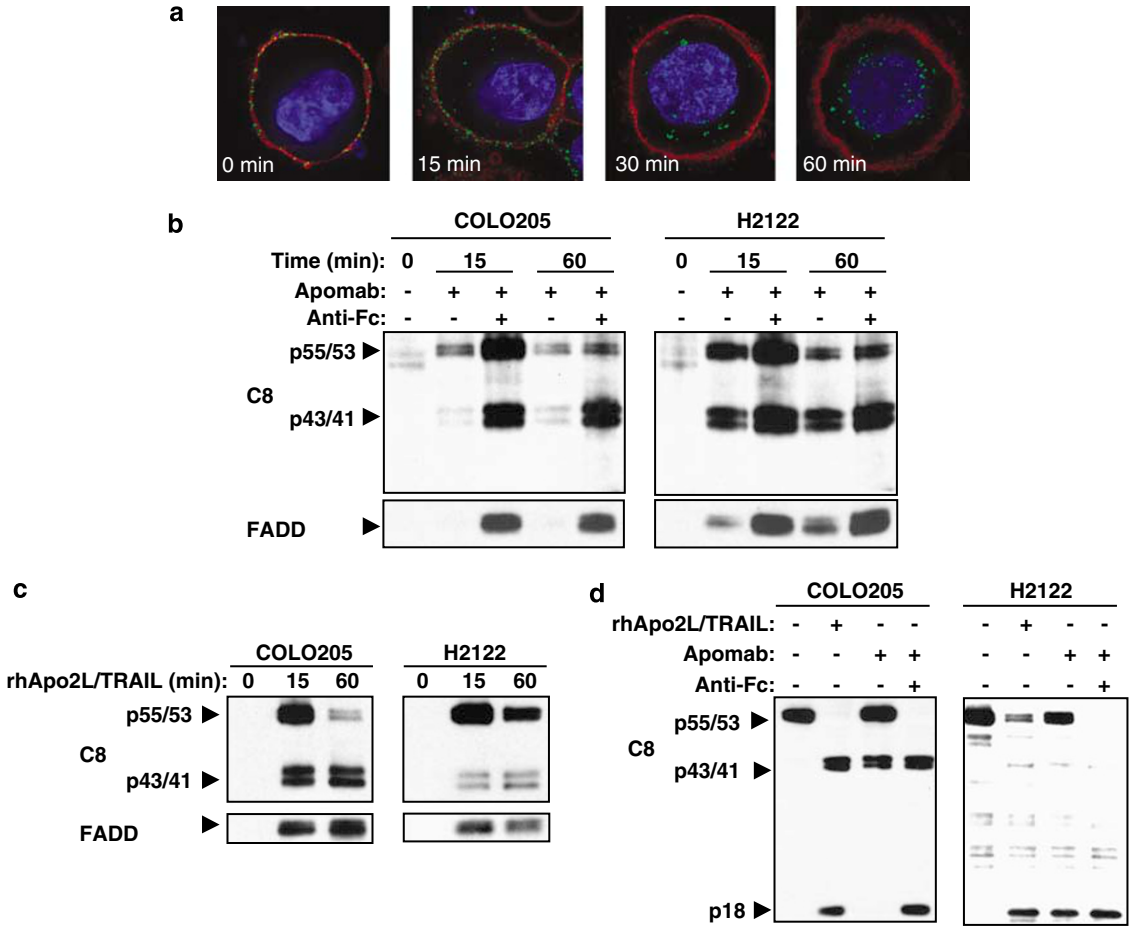

Figure 3 Apomab induces DR5 clustering and DISC activation. (**a**) H460 NSCLC cells were grown on glass coverslips and incubated with Apomab (2 μg/ml, 1 h on ice), followed by Cy3-labeled anti-human IgG antibody (5 μg/ml, 1 h on ice). The cells were transferred to 37°C for the indicated time and stimulation was stopped by cold PBS wash. The plasma membrane was visualized by staining with Alexa-488-labeled cholera toxin subunit B (1 μg/ml, 10 min on ice). The cells were fixed in 4% paraformaldehyde, mounted on slides using DAPI-containing mounting media and analyzed by deconvolution microscopy. Cy3, green; Alexa-488, red and DAPI, blue. COLO205 colorectal cancer cells or H2122 NSCLC cells were treated with Apomab (10 μg/ml) alone or in combination with anti-human Fc antibody (10 μg/ml) (**b**) or recombinant human (rh) Apo2L/TRAIL (1 μg/ml) (**c**) for the indicated time at 37°C, and stimulation was stopped by cell lysis. (**b**, **c**) The cells were lysed in a buffer containing 1% Triton X-100 and cleared cell lysates were subjected to immunoprecipitation with anti-DR5 monoclonal antibody 5C7 (which does not compete with Apomab or Apo2L/TRAIL) coupled to protein G sepharose. Immunoprecipitates were analyzed by SDS-PAGE (10% acrylamide gels), and caspase-8 (C8) and FADD proteins that co-immunoprecipitated with DR5 were visualized by immunoblot analysis. The 5F7 caspase-8 antibody used for DISC analysis recognizes the p55/53 full-length and the p43/41-cleaved intermediate of caspase-8 (see arrows). (**d**) Cells were treated with Apomab as in (**b**) or rhApo2L/TRAIL as in (**c**) for 4 h at 37°C, lysed in a buffer containing 1% NP40, and cleared cell lysates were directly analyzed by SDS-PAGE and caspase-8 immunoblot to detect total cellular caspase-8. The 1C12 caspase-8 antibody used for analysis of cell lysates detects the full-length and cleaved intermediate as well as the cleaved p18 subunit (arrows)

of effector caspases as determined by a caspase-3/7 substrate conversion assay (Figure 4b). Similar to the DISC results, anti-Fc crosslinking further augmented the stimulation of cell death and of caspase-3/7 activity, shifting the Apomab dose–response curves to lower concentrations (Figure 4a and b). Apomab exerted similar activity on H2122 NSCLC cells (Figure 4c and d).

In contrast to its proapoptotic activity against these cancer cell lines, Apomab showed no effector caspase activation or cell death induction in normal human hepatocytes, even upon anti-Fc crosslinking (Figure 4e and other data not shown).

***In vivo* antitumor activity of Apomab as a single agent.** To assess the effect of Apomab on the growth of human tumor xenografts *in vivo*, we used a panel of cell lines from colorectal, lung and pancreatic cancer that expressed cell surface DR5 as measured by flow cytometry (Supplementary Figure 6c). In the first study, we treated Nu/nu mice bearing pre-established subcutaneous COLO205 tumors. We injected the mice i.p. once per week over 3 weeks with Apomab or vehicle and followed tumor volumes for 34 days (Figure 5a). At doses of 0.1 and 0.3 mg/kg, Apomab caused a delay in tumor progression. In contrast, at 1 and 10 mg/kg, Apomab induced substantial tumor regression and a greater delay in tumor re-growth, or an apparent tumor ablation in some mice. Several complete responses (CRs, defined as complete tumor regression at any time during treatment as compared to tumor volume at treatment initiation) were observed, reaching 7 of 9 animals at both the 3 and 10 mg/kg Apomab dose levels. On day 34, 2 of 8 animals in the 1 mg/kg dose group, 3 of 9 animals in the 3 mg/kg dose group and 6 of 9 animals in the 10 mg/kg dose group remained free of palpable

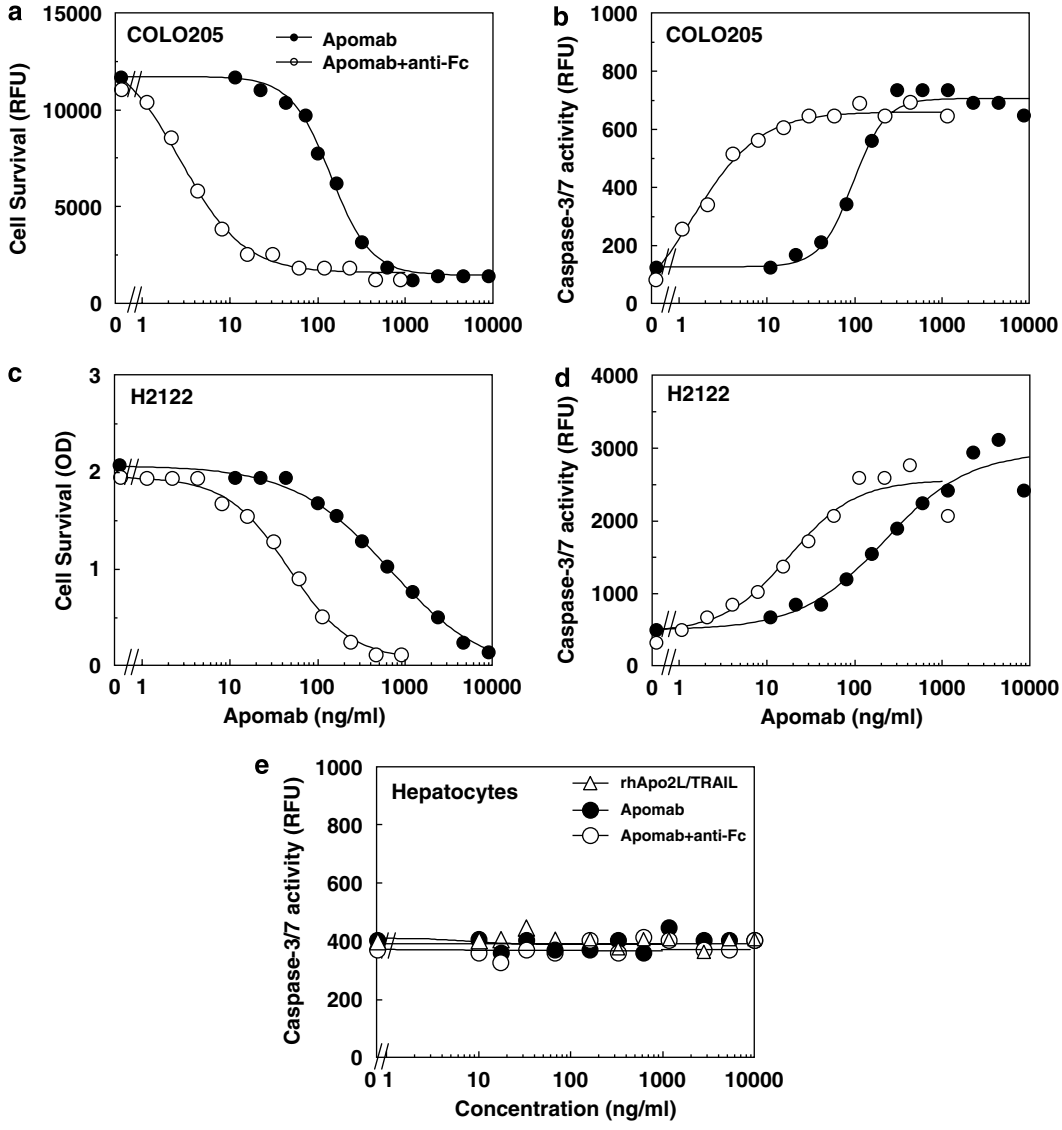

Figure 4 Proapoptotic activity of Apomab *in vitro*. (**a**, **b**) COLO205 colorectal cancer cells. (**c**, **d**) H2122 NSCLC cells. Cells were treated with Apomab (from 1 ng/ml to 10 μg/ml) alone or in combination with anti-human Fc antibody (10 μg/ml) for 48 h and cell survival (**a**, **c**, analysis by AlamarBlue or crystal violet assay) or caspase-3/7 enzymatic activity (**b**, **d**, determined by a substrate conversion assay) was analyzed. The first data point in each curve represents treatment in the absence of Apomab. (**e**) Primary cynomolgus monkey hepatocytes were treated as in (**a**–**d**) for 48 h with Apomab with or without anti-Fc antibody or with recombinant human (rh) Apo2L/TRAIL, followed by analysis of caspase-3/7 activity by substrate conversion assay

tumors. Histologic analysis of COLO205 tumor sections from a separate set of animals demonstrated that Apomab induced apoptosis in a substantial fraction of tumor cells within 48 h of dosing (Figure 5b). We next tested the efficacy of a single intravenous (i.v.) Apomab administration (Figure 5c). Apomab elicited tumor regression followed by a marked delay in tumor progression. A CR was seen in 7 of 8 animals in the Apomab dose group; on day 30, 5 of 8 animals in this group were still free of palpable tumors.

To extend these studies to a second type of cancer, we examined the effect of Apomab on the growth of established s.c. H2122 NSCLC tumor xenografts (Figure 5d). Nu/nu mice bearing s.c. tumors of $\sim$175 mm^3 were given a single i.v. injection of vehicle or various Apomab doses, and tumor volume was followed for 32 days. In a dose-dependent manner, Apomab induced a substantial tumor regression, which was either followed by a marked delay in re-growth or sustained. A CR was observed in 6 of 9 animals in the 1 mg/kg Apomab dose group, 8 of 9 animals in the 3 mg/kg dose group and 9 of 9 animals in the 10 mg/kg dose group. On day 32, 5 of 9 animals in the 1 mg/kg Apomab dose group, 8 of 8 animals in the 3 mg/kg dose group and 9 of 9 animals in the 10 mg/kg dose group remained free of palpable tumors.

Next, we examined the activity of Apomab against Mia-PaCa-2 pancreatic tumor xenografts (Figure 5e). Nu/nu mice bearing s.c. tumors of $\sim$125 mm^3 were given a single i.v. injection of vehicle or Apomab at 10 mg/kg, and tumor volumes were followed for 32 days. Apomab induced a

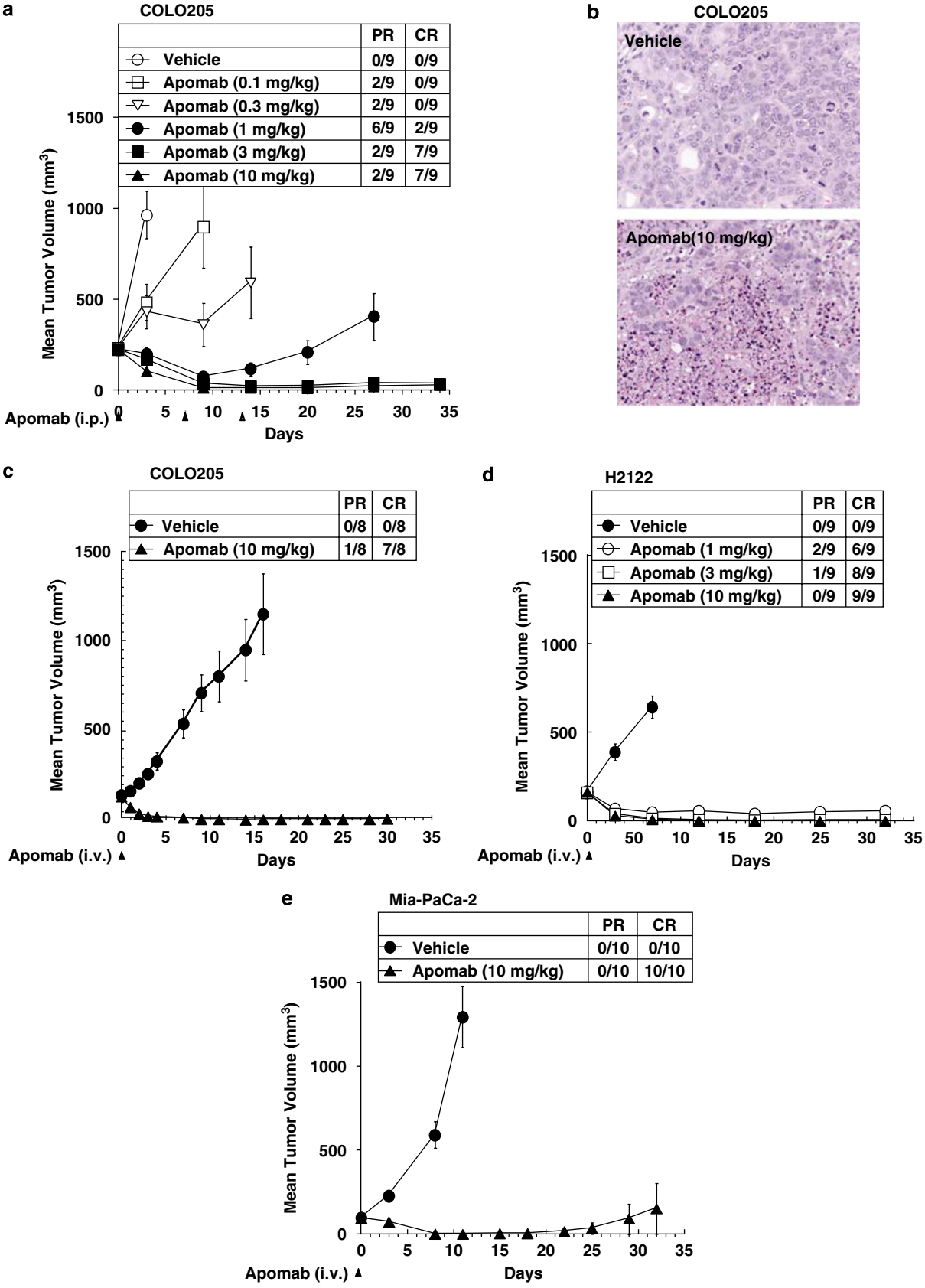
a
COLO205
PR CR
Vehicle 0/9 0/9
Apomab (0.1 mg/kg) 2/9 0/9
Apomab (0.3 mg/kg) 2/9 0/9
Apomab (1 mg/kg) 6/9 2/9
Apomab (3 mg/kg) 2/9 7/9
Apomab (10 mg/kg) 2/9 7/9
Mean Tumor Volume (mm3)
Apomab (i.p.)
Days
b
COLO205
Vehicle
Apomab(10 mg/kg)
c
COLO205
PR CR
Vehicle 0/8 0/8
Apomab (10 mg/kg) 1/8 7/8
Mean Tumor Volume (mm3)
Apomab (i.v.)
Days
d
H2122
PR CR
Vehicle 0/9 0/9
Apomab (1 mg/kg) 2/9 6/9
Apomab (3 mg/kg) 1/9 8/9
Apomab (10 mg/kg) 0/9 9/9
Mean Tumor Volume (mm3)
Apomab (i.v.)
Days
e
Mia-PaCa-2
PR CR
Vehicle 0/10 0/10
Apomab (10 mg/kg) 0/10 10/10
Mean Tumor Volume (mm3)
Apomab (i.v.)
Days

marked tumor regression, which was either followed by a delay in re-growth or sustained. CR was observed in 10 of 10 animals in the Apomab dose group. On day 32, 9 of the 10 animals treated with Apomab remained free of palpable tumors. These results show that Apomab can exert potent activity against susceptible tumor xenografts *in vivo*.

Interaction of Apomab with chemotherapy. To examine whether Apomab may cooperate with chemotherapy, we selected cancer cell lines that expressed DR5, yet were less sensitive to apoptosis induction by the antibody *in vitro* (Supplementary Figure 6d and data not shown), and tested the *in vivo* efficacy of Apomab in combination with relevant chemotherapy agents. For colorectal cancer xenografts, we used irinotecan hydrochloride (CPT-11), which is an approved chemotherapy for this cancer. Nu/nu nude mice bearing s.c. HCT-15 tumor xenografts of $\sim$180 mm^3 were treated either with vehicle, or a single i.v. dose of Apomab alone (10 mg/kg), or CPT-11 alone (80 mg/kg i.p. on days 0, 4 and 8), or both the Apomab and CPT-11 regimens. Tumor volume was followed over 32 days (Figure 6a). CPT-11 monotherapy delayed tumor progression and resulted in 1 of 10 partial responses (PRs) but no CRs. Apomab monotherapy caused detectable tumor regression and resulted in a PR in 5 and a CR in 2 of the 10 mice. Combination therapy with Apomab and CPT-11 resulted in a more substantial tumor regression, with a PR in 2 and a CR in 8 of the 10 animals. Treatment of mice bearing LS180 colon tumor xenografts of $\sim$180 mm^3 with Apomab or CPT-11 only slightly delayed mean rates of tumor growth (Figure 6b); however, the combination of both agents led to tumor regression and a significant delay in tumor re-growth. Similarly, treatment of mice bearing DLD-1 s.c. colon tumor xenografts of $\sim$200 mm^3 with Apomab or CPT-11 monotherapy delayed tumor growth, while the combination of both agents led to strong tumor regression, with a PR in three and a CR in five of eight animals (Figure 6c). We also studied pancreatic tumor xenografts, using gemcitabine, which is an approved chemotherapy agent for this cancer. Treatment of mice bearing BxPC-3 pancreatic cancer xenografts of $\sim$150 mm^3 with gemcitabine alone caused a slight delay in tumor growth, while Apomab monotherapy exerted a more substantial antitumor effect with a PR in 5 of 10 mice (Figure 6d). While the combination of both agents similarly inhibited the change in mean tumor volume as did Apomab monotherapy, it showed a greater number of responses, namely, a PR in 7 and a CR in 1 of 10 mice (Figure 6d). These studies demonstrate that the combination of Apomab with certain chemotherapeutic agents can lead to cooperative or additive activity against tumor xenografts.

Discussion

The extrinsic apoptosis pathway is an intriguing target for cancer therapy because it can circumvent a common apoptosis resistance mechanism associated with inactivation of p53 in cancer cells.[3] The proapoptotic receptors DR4 and DR5 are of unique interest because initiation of apoptosis through these receptors appears to display remarkable selectivity for malignant *versus* normal cells. Two types of PARAs directed toward DR4 and/or DR5 that are currently in clinical trials are rhApo2L/TRAIL[21] and various agonistic DR4 or DR5 monoclonal antibodies.[6,24–27,32,36] (see also www.clinicaltrials.gov). Although the structure of Apo2L/TRAIL alone and in complex with the extracellular region of DR5 has been described in several different publications,[33,34,37,38] little information has been reported in the scientific literature as to the structure of DR5 agonistic antibodies in complex with the DR5 protein. Here, we used a novel, fully human agonistic monoclonal DR5 antibody to examine further structural and functional aspects of antibody-mediated activation of DR5.

Our binding studies confirmed that Apomab associates with high affinity (K_D $\sim$0.9 nM) with its target – human DR5. The interaction was selective since Apomab binding to other Apo2L/TRAIL receptors, namely, DR4, DcR1, DcR2 or OPG was not detectable. The X-ray crystallographic structure of the Apomab Fab in complex with DR5 revealed that the binding sites for Apomab and the endogenous DR5 ligand Apo2L/TRAIL on DR5 are overlapping, although the ligand's contact site is divided into two patches while the region that Apomab contacts is more continuous. Like Apo2L/TRAIL, Apomab interacts with residues in CRD2 as well as CRD3. In contrast, another DR5 antibody called BDF1 that we have characterized as having little or no agonistic activity interacts with CRD2 but not CRD3. The importance of the specific antibody epitope on DR5 may reflect a need to cluster the pre-associated receptor oligomers in a particular orientation to permit optimal recruitment of DISC components; different structural epitopes also may impact the availability of the Fc portion of the antibody for additional crosslinking (see Figure 7 for a schematic model). Consistent with the latter ideas, the orientation of CRD3 with respect to CRD1 and CRD2 showed conformational diversity in independent structures of DR5 bound to either ligand or antibody Fab fragments, suggesting that this region is dynamic *in vivo* and may be stabilized by Apomab in a specific arrangement that promotes DR5 activation.

Immunofluorescence experiments indicated that Apomab stimulates clustering of DR5 at the cell surface as well as receptor internalization. These findings are similar to the effects of rhApo2L/TRAIL on DR5.[35] Immunoprecipitation of

Figure 5 Antitumor activity of Apomab as a single agent *in vivo*. (**a**) Effect of i.p. treatment with Apomab (0.1–10 mg/kg; days 0, 7 and 14) on the growth of established s.c. COLO205 colon cancer xenografts. Nu/nu mice were injected subcutaneously with COLO205 cells and tumors were allowed to grow to a mean volume of $\sim$250 mm^3. Mice were then randomly assigned into groups and treated with vehicle or the indicated doses of Apomab on days 0, 7 and 14 after randomization. (**b**) Representative hematoxylin and eosin-stained sections from the study in (**a**) indicating frequent apoptotic cell morphology at 48 h after treatment with Apomab (10 mg/kg). (**c**) Effect of i.v. treatment with Apomab (10 mg/kg; day 0) on the growth of established s.c. COLO205 xenografts. Mice were injected with COLO205 cells as in (**a**) and treated upon randomization with a single i.v. injection of vehicle or Apomab. (**d**) Effect of i.v. treatment with Apomab (1–10 mg/kg; day 0) on the growth of established s.c. H2122 NSCLC xenografts. Mice were injected with H2122 cells and tumors were allowed to grow to a mean volume of $\sim$200 mm^3. Mice were then randomly assigned into groups and treated with a single i.v. injection of vehicle or the indicated doses of Apomab. One animal in the 1 mg/kg dose group was euthanized early because of tumor ulceration. (**e**) Effect of i.v. treatment with Apomab (10 mg/kg; day 0) on the growth of established s.c. Mia-PaCa-2 pancreatic tumor xenografts. Mice were injected with Mia-PaCa-2 cells and tumors were allowed to grow to a mean volume of $\sim$125 mm^3. Mice were then randomly assigned into groups and treated with a single i.v. injection of vehicle or Apomab

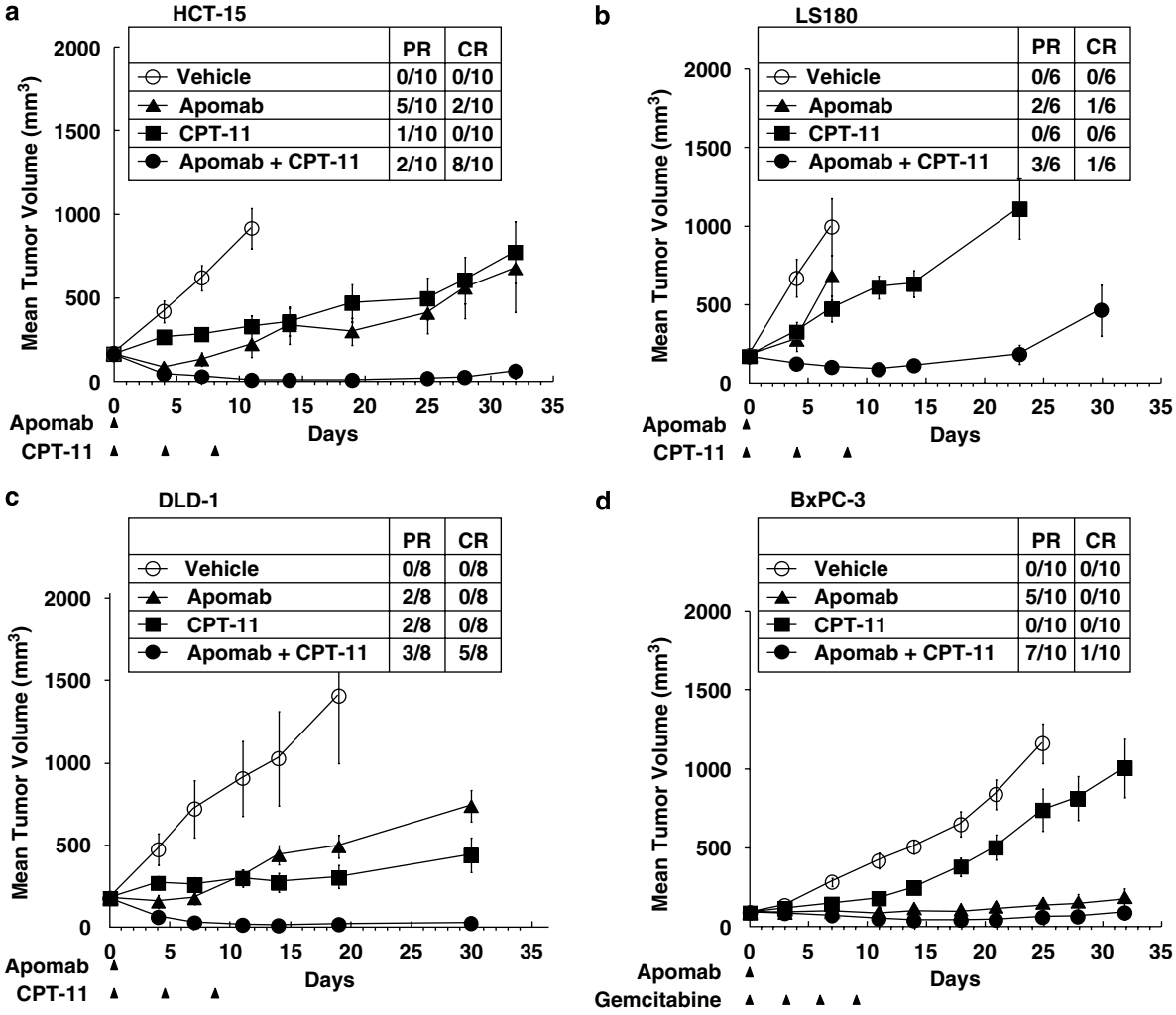

Figure 6 Antitumor activity of Apomab in combination with chemotherapy *in vivo*. (**a**–**c**) Effect of Apomab (10 mg/kg i.v.; day 0), or CPT-11 (80 mg/kg i.p.; days 0, 4 and 8), or the combination of both treatments on the growth of established s.c. HCT-15 (**a**), LS180 (**b**) or DLD-1 (**c**) colon tumor xenografts. (**d**) Effect of Apomab (10 mg/kg i.v.; day 0), or gemcitabine (160 mg/kg i.p.; days 0, 3, 6 and 9), or the combination of both treatments on the growth of established s.c. BxPC-3 pancreatic tumor xenografts. Mice were injected subcutaneously with the indicated tumor cells and randomized into treatment groups when mean tumor volume reached 50–200 mm^3, and treated with Apomab, CPT-11, gemcitabine or combinations thereof as indicated

DR5 from stimulated cells showed that Apomab induces recruitment of FADD and caspase-8 to DR5, leading to the assembly of a DISC and to processing of caspase-8, which indicates its activation. These results show that similar to rhApo2L/TRAIL, Apomab initiates apoptosis through the extrinsic pathway. Apomab alone displayed agonistic activity toward DR5, and experimental data revealed that this function was further augmented by anti-Fc crosslinking, consistent with the hypothesis that super-clustering of DR5 may have the ability to further enhance apoptosis signaling (Figure 7).

Our *in vitro* experiments demonstrated that Apomab can induce apoptosis in various cancer cell lines, as indicated by loss of cell viability in conjunction with effector caspase activation. Hepatocytes have been noted as a normal cell type that can be susceptible to apoptosis activation by FasL, or several non-optimized Apo2L/TRAIL preparations,[39,40] or certain DR4 or DR5 antibodies.[41] We found that Apomab did not stimulate any detectable caspase activation in cultured hepatocytes, whether or not it was crosslinked by an anti-Fc antibody. Hence, it is anticipated that administration of this antibody to humans is unlikely to have adverse effects on the liver. Further support for this conclusion comes from safety studies in cynomolgus monkeys (Genentech Inc., data on file).

The *in vivo* studies showed that Apomab is capable of exerting potent antitumor activity in various xenograft models of cancer, including colorectal cancer, NSCLC and pancreatic ductal cancer. Significant subsets of animals in the various studies showed regression of established tumors in response to Apomab treatment, attesting to the strong efficacy of the antibody in these models. Moreover, Apomab showed a positive interaction with irinotecan against two colon cancer xenografts and with gemcitabine against a pancreatic tumor xenograft. These results suggest that it may be possible to harness the proapoptotic activity of DR5 agonistic antibodies such as Apomab across a range of tumor types and treatment regimens. It is notable that while many of the cancer cell lines

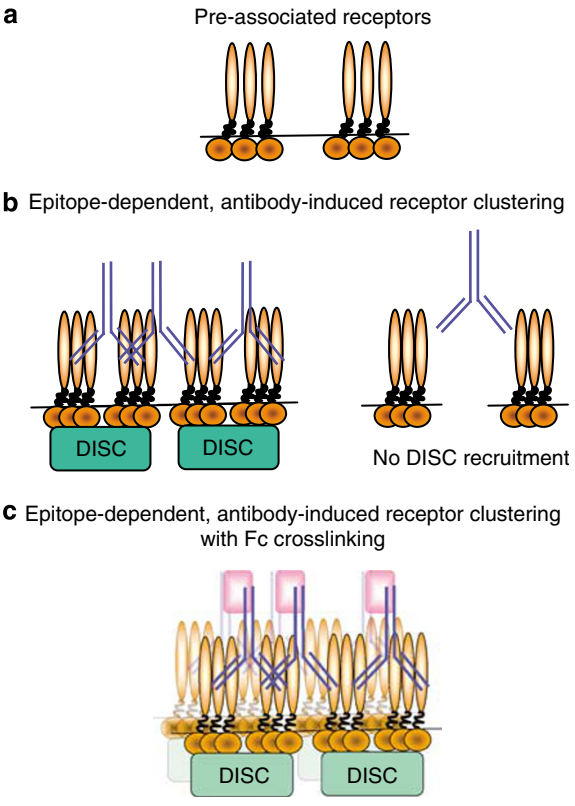

Figure 7 Model of antibody-induced DR5 signaling. (**a**) Before engagement by antibody, receptors (orange) are pre-associated in small oligomers but non-signaling. (**b**) Antibody (blue) engagement promotes clustering of pre-associated receptors, and this leads to signal-competent complexes that can recruit DISC components in an epitope-dependent manner. (**c**) Addition of anti-Fc (pink) can further crosslink and hence stabilize the signal-competent clusters, enhancing apoptosis signaling. The location of the antibody epitope on DR5 appears to influence steps (**b** and **c**): epitopes that overlap with the ligand-binding site appear to favor receptor activation

we studied express both DR4 and DR5, activation of DR5 was sufficient to achieve marked efficacy. This result agrees with earlier studies assessing the proapoptotic activity of receptor-selective rhApo2L/TRAIL mutants against solid tumor-derived cell lines.[42] On the other hand, it has recently been reported that there may be certain types of leukemia, for example, chronic lymphocytic leukemia, in which DR4 activation may be more important to achieve significant efficacy.[43] Notwithstanding, there may also even be some clinical scenarios in which engaging both DR4 and DR5 to affect proapoptotic signals could be advantageous. Recent studies have revealed that expression of certain O-glycosylation enzymes on cancer cells may provide a strong predictor of sensitivity to rhApo2L/TRAIL in association with O-glycan modification of DR4 and DR5.[44] Further information on the safety and efficacy of such proapoptotic molecules will be obtained as they continue to be evaluated in clinical settings. In such trials, analysis of the levels of target receptors and/or other biomarkers may be helpful in determining clinical outcome in human cancer patients. In conclusion, our results provide new insight into the structure of the complex between Apomab and DR5 and demonstrate that Apomab stimulates DR5-mediated apoptosis effectively in cancer cells both *in vitro* and *in vivo*, supporting further investigation of this antibody for cancer therapy.

Materials and Methods

Cell lines and reagents. The human cell lines NCI-H460, COLO 205, NCI-H2122, Mia-PaCa-2, HCT-15, LS180, DLD-1 and BxPC-3 were obtained from American Type Cell Culture Collection. Cell lines were maintained in RPMI medium supplemented with L-glutamine and 10% fetal bovine serum (Invitrogen Inc., Carlsbad, CA, USA) under conditions of 5% CO_2 at 37°C. Cynomolgus hepatocytes were purchased from CellzDirect Inc. (Pittsboro, NC, USA) and used directly in the assay. Goat F(ab′)2 anti-human immunoglobulin (Ig) G Fc was purchased from Pierce (Rockford, IL, USA). Fc fusion proteins consisting of the extracellular portion of DR4, DR5, DcR1, DcR2 and OPG linked to the hinge and Fc regions of human IgG1 were generated as described previously.[45–47]

Generation of Apomab. The variable domains of a first variant of Apomab were derived as single-chain Fv (scFv) from a human antibody phage display library (Genentech Inc., South San Francisco, CA, USA). Phage were blocked with unlabeled DR4-Fc, DcR1-Fc and CD4-Fc in a solution of MPBST (3% dry milk powder, 1 × PBS, 0.2% Tween) to derive antibodies specific for DR5. Biotinylated DR5-Fc was then added and phage allowed to bind for 1 h at 37°C. The DR5-specific phage, non-covalently bound to the biotinylated antigen, were captured on streptavidin-coated DYNABEADS M-280 (*Dyna*l; Invitrogen Inc.) and pulled out of the solution with a magnet. The beads were washed 4–6 times with MPBST and PBS-Tween and remaining phage eluted with triethylamine. Neutralized phage were used to infect mid-log *Escherichia coli* for rescue and induction of phage for subsequent rounds of panning. After the third round, phages were screened for binding to DR5-Fc (but not human IgG1 Fc) by ELISA. Positive clones were screened in scFv format for agonistic activity against COLO205 cells by crystal violet cell viability assay and secondary apoptosis assays including caspase-3/7 activity. scFvs with proapoptotic activity were reformatted as full-length antibodies and re-assayed. The clone with the most potent activity was selected for further modifications and affinity maturation. Variants of the lead clone were constructed on the light or heavy chains separately using site-directed mutagenesis.[48] Alanine scanning mutagenesis was performed on each CDR separately to determine which residues could be changed to improve affinity. In addition, for each CDR of the light chain, a phage display library randomizing all residues was constructed, and panning on biotinylated DR5-Fc was carried out as described above, with increasing stringency of washing in each round. Each variant constructed was transiently expressed as an IgG1/λ3 in HEK293 cells and purified by protein A chromatography. Binding was determined as described below. These changes in the light chain that separately gave improvements in binding, or were predicted to improve chemical or thermal stability, were combined into several light-chain variants. Likewise, combination variants of the heavy chain were constructed. The light- and heavy-chain versions were then transfected pairwise into HEK293 cells for protein production, and the resulting variants were again assayed. Clones with the best affinity and potentially improved stability were compared for potency in tumor xenograft studies and for lack of activity against cultured cynomolgus monkey hepatocytes, leading to the selection of a desired variant that was dubbed Apomab.

Binding studies. A direct-binding ELISA was used to evaluate the specificity of binding of Apomab to a panel of Apo2L/TRAIL receptors. Purified human IgG1 Fc fusion proteins (DR4, DR5, DcR1, DcR2 and OPG) were coated overnight onto 384-well ELISA plates (Nunc, Neptune, NJ, USA). After the plates were blocked with PBS/0.5% BSA, a serial dilution of Apomab was added. Bound Apomab was detected using a horseradish peroxidase-conjugated goat $F(ab')_2$ anti-human IgG $F(ab')_2$ antibody (Jackson ImmunoResearch, West Grove, PA, USA). The plates were developed using tetramethyl benzidine (Kirkegaard & Perry Laboratories, Gaithersburg, MD, USA), and the reaction was stopped using 1 M H_3PO_4. The plates were read at 450 nm with a 620 nm reference. Competitive binding of Apomab to DR5 was assessed using an electrochemiluminescent (ECL) solution-phase assay. Human DR5-Fc was biotinylated using Biotin-X-NHS (Research Organics, Cleveland, OH, USA) and Apomab was conjugated to a ruthenium chelate (BV-TAG) according to the manufacturer's instructions (BioVeris Corporation, Gaithersburg, MD, USA). Fixed concentrations of biotin-DR5-Fc and TAG-Apomab were incubated with a dilution series of unlabeled Apomab for 2 h at room temperature. Streptavidin magnetic beads (BioVeris Corporation) were added

and, after 30 min incubation, the plates were read in a BioVeris M384 analyzer to detect the ECL signal derived from intact complexes of biotin-DR5-Fc and TAG-Apomab. The dissociation constant (K_D) for binding of Apomab to DR5-Fc was measured at room temperature by saturation binding analysis as follows: microtiter plates (96-well) with removable wells (Nunc) were coated overnight with goat anti-human IgG at 5 μg/ml (Jackson ImmunoResearch) and blocked for 1 h with PBS/1.0% BSA. The plates were washed with PBS/0.05% Tween-20 and then incubated with 5 μg/ml DR5-Fc in PBS/0.5% BSA/0.05% Tween-20 for 1 h. Radio-iodination was carried out using the lactoperoxidase method and labeled Apomab was prepared for the assay at a specific activity of 12.3 μCi/μg. Total ^{125}I-Apomab binding was determined in duplicate in a 96-well plate containing increasing concentrations of ^{125}I-Apomab in the incubation buffer for 60 min at room temperature. In a separate set of reactions, unlabeled Apomab was added at a concentration of 3.3 μM to the reactions with labeled Apomab to determine nonspecific binding. The plates were then washed four times and the bound ^{125}I-Apomab was measured with a Wallac gamma counter (Perkin Elmer, Waltham, MA, USA). Specific ^{125}I-Apomab binding was then calculated by subtracting the nonspecific binding from the total c.p.m. bound. Data were analyzed with nonlinear one-site curve fit using Prism software (GraphPad, San Diego, CA, USA).

Crystallization, structure determination and refinement. The human DR5-ECD (residues 1–130) was purified as described.[33] The Apomab Fab was expressed in *E. coli* and purified over a protein G affinity column.[49,50] Fab-containing fractions were further purified by passage over a SP-Sepharose column (Pharmacia). Apomab–DR5 complex was generated by incubating Apomab with an excess of DR5-ECD followed by purification over a Superdex-200 sizing column. The complex-containing fractions were pooled and concentrated to 7 mg/ml in 20 mM Tris-HCl pH 8.0 and 150 mM NaCl and used for crystallization trials. Crystals grew at 19°C from hanging drops containing an equal volume of protein and well solution consisting of 30% polyethylene glycol 4K, 0.1 M Tris-HCl pH 8.5 and 0.2 M $MgCl_2$. The crystals were cryo-protected by immersion in crystallization buffer with 40% PEG 3350 and then cooled in liquid nitrogen. Data was collected at ALS beam line 5.0.2 and processed with XDS. The structure was solved in space group P6 by molecular replacement with the program AMoRe using the structure 8FAB as a search model. The resulting maps showed clear density for hDR5-ECD (from pdb 1d0g, chain S), which were placed manually, as well as for the Apomab CDRs. Refinement was performed with the program REFMAC5 and included TLS refinement. A Ramachandran plot shows that the model has good geometry with 98.3% of residues in the most favored or additionally allowed regions with only 1.2% in generously allowed and 0.5% in the disallowed regions.

Immunofluorescence analysis. H460 cells were selected for immunofluorescence studies because they are strongly adherent. Cells were grown on glass coverslips in tissue culture dishes and transferred to ice. The cells were treated with Apomab (2 μg/ml) for 1 h on ice, washed with cold PBS and stained with Cy3-conjugated anti-human IgG (Jackson ImmunoResearch) for 1 h on ice and washed with PBS. Samples were transferred to a 37°C water bath in a 37°C/5% CO_2 tissue culture incubator for the times indicated and returned to ice. Cells were washed twice with cold PBS and stained with Alexa-488-labeled cholera toxin subunit B (Invitrogen Inc.) (1 μg/ml) for 10 min on ice to label the plasma membrane. Samples were washed three times with cold PBS and fixed with 4% paraformaldehyde and the coverslips mounted on glass slides using mounting media with DAPI to allow visualization of the nuclei. Images were taken on an Olympus IX70 wide-field inverted fluorescence microscope using an Olympus UPlanApo $\times$ 100, NA 1.35, oil immersion objective. Serial *Z*-section images were captured using the DeltaVision image acquisition system (Applied Precision, Issaquah, WA, USA) with a Photometrics CCD camera (Roper Scientific, Tuscon, AZ, USA). The *Z*-stacks were deconvolved and maximum intensity projections were created using Softworx imaging software (Applied Precision). Images were assembled using Photoshop (Adobe Systems Inc., San Jose, CA, USA).

DISC analysis, cell lysate analysis and immunoblot. COLO205 or H2122 cells (1×10^7 per time point) were treated with Apomab (10 μg/ml) or Apomab crosslinked by anti-human Fc (Pierce; 10 μg/ml each). For DISC analysis, incubation for the indicated time was carried out at 37°C. Stimulation was stopped by putting cells on ice and washing two times in cold PBS. Cells were collected by centrifugation, lysed in a buffer containing 20 mM Tris-HCl, 150 mM NaCl, 10% glycerol, 2 mM EDTA, 0.57 mM PMSF, 1% Triton X-100, immunoprecipitated with protein G conjugated (Pierce) anti-DR5 monoclonal antibody 5C7[35] (which does not compete with Apomab or Apo2L/TRAIL) and analyzed by immunoblot. For analysis of caspase-8 processing in cell lysates, incubation was carried out as above for 4 h and the cells were collected and lysed in the same buffer containing 1% NP40 rather than Triton X-100. For immunoblot analysis of the immunoprecipitated DISC, anti-caspase-8 5F7 (Immunotech, Marseille, France) and anti-FADD (BD Transduction, Billerica, MA, USA) were used. (The 5F7 antibody does not have cross-reactivity with the IgG heavy chain so it is preferable for caspase-8 immunoblot of immunoprecipitates.) For direct immunoblot analysis of cell lysates, anti-caspase-8 1C12 (Cell Signaling) was used. The following secondary horseradish peroxidase-conjugated antibodies were used: anti-mouse-IgG1 (BD Bioscience) and anti-mouse-IgG2b (Southern Biotechnology, Birmingham, AL, USA). Anti-rabbit-IgG and strepavidin were from Jackson ImmunoResearch. Immunoprecipitated proteins or cleared cell lysates were run on 10% NuPAGE gels (Invitrogen Inc.).

Cell viability and caspase-3/7 activity assays. AlamarBlue™ (Accumed International Inc., Chicago, IL, USA) or crystal violet assay was used to determine cell viability after a 48 h treatment with serial dilutions of Apomab. Cells were seeded and treated in 96-well plates in a 37°C/5% CO_2 incubator. For AlamarBlue assay, fluorescence was read by fluorometer with excitation at 530 nm and emission at 590 nm. For the crystal violet assay, the cells were seeded and treated similarly, and the medium was removed. Then, 100 μl of 0.5% crystal violet solution was added to each well and incubated at room temperature for 10 min, followed by washing with water. After the wells were dry, 100 μl of ethanol containing 0.5 N HCL was added and the plates were read at 540 nm. Each assay was run in triplicate; a four-parameter curve fit was used for data analysis. Analysis of caspase-3/7 activity was performed using the Apo-ONE homogenous caspase-3/7 assay (Promega, Madison, WI, USA). Cells were incubated with Apomab for 24 h before lysis and addition of a fluorescent caspase substrate.

Tumor xenograft studies. Female Nu/nu mice (Charles River Laboratory, Hollister, CA, USA) 6–8 weeks of age were injected with 5×10^6 cells per mouse of human colorectal cancer COLO205, HCT-15, LS180, DLD-1 or human NSCLC H2122 cells subcutaneously in a volume of 0.2 ml in HBSS. Tumors were measured in two dimensions using a caliper. Tumor volume was calculated using the formula: $V = 0.5a \times b^2$, where *a* and *b* are the long and the short diameters of the tumor, respectively. Data collected from each experimental group were expressed as mean $\pm$ S.E. Once the mean tumor volume reached 100–250 mm^3, mice were randomly assigned into groups of 6–10 mice and treatment was administered either intraperitoneally or intravenously with vehicle (0.5 M arginine succinate/20 mM Tris/0.02% Tween-20 pH 7.2 or 10 mM histidine/8% sucrose/0.02% Tween-20 pH 6), Apomab (0.1–10 mg/kg), CPT-11 (Camptosar, Pharmacia & Upjohn; 80 mg/kg, once every 4 days $\times$ 3), or the combination of Apomab and CPT-11. In studies utilizing chemotherapy, body weights were monitored using a calibrated scale. A PR is defined as a reduction of tumor volume of at least 50% but less than 100% and a CR as a reduction of 100% at any time during treatment as compared with the initial tumor volume as determined at the start of treatment. For the human ductal pancreatic adenocarcinoma transplant xenograft models BxPC-3 and Mia-PaCa-2 tumor (Piedmont Research Center, Morrisville, NC, USA), female Nu/nu mice (Harlan Sprague Dawley Inc., IN, USA) received a 1-mm^3 tumor fragment subcutaneously in the right flank, and tumor growth was monitored using a caliper. Once the tumors reached an average size of 60–130 mm^3, mice were randomly grouped into 9 or 10 mice per group, then treatment was administered with vehicle (i.p.), Apomab (i.v.) at 10 mg/kg or gemcitabine (i.p.) (Gemzar, Eli Lilly and Company) at 160 mg/kg, once every 3 days $\times$ 4.

In all experiments, mice were euthanized before mean tumor volumes reached 2000 mm^3 or in some instances mice were euthanized earlier in the course of the study due to tumor ulcerations. All the experimental procedures were approved by Genentech's Institutional Animal Care and Use Committee or the *Guide for Care and Use of Laboratory Animals* with respect to restraint, husbandry, surgical procedures, feed and fluid regulation, and veterinary care. The animal care and use programs are also accredited by the Association for Assessment and Accreditation of Laboratory Animal Care, which assures compliance with accepted standards for the care and use of laboratory animals. For histological analysis, tumor tissue was excised and placed into neutral-buffered formalin for overnight fixation at room temperature. Tissues were then processed into paraffin blocks and 5-μm-thick sections were stained with hematoxylin and eosin for microscopic evaluation of tumor morphology and presence of apoptotic activity.

Flow cytometry. Cells (10^6) were washed once with PBS and suspended in 1 ml FACS buffer ($1\times$ PBS, 3% FBS) containing 2 μg/ml primary antibody (anti-DR4 4H6 or anti-DR5 3H3; Genentech Inc.). Cells were stained on ice for 60 min, then washed with 3 ml cold FACS buffer and incubated with the secondary antibody (1 : 100 dilution FITC-conjugated goat anti-mouse $F(ab')_2$ anti-IgG + IgM (Jackson ImmunoResearch) for 60 min, on ice, in the dark. After an additional wash with 3 ml cold PBS, cells were suspended in 1 ml cold FACS buffer and 10 000 cells per sample were analyzed using an Elite-ESP flow cytometer (Beckman-Coulter, Miami, FL, USA).

Acknowledgements. We thank Roger Pai and Jim Andya for purification and formulation of Apomab, Susan Spencer for coordination of xenograft studies and Linda Mosqueda for editorial assistance. This paper is dedicated to the memory of Ralph Schwall and the memory of Suzan Palmieri, both of whom made important contributions to this study.

1. Ferlay J, Autier P, Boniol M, Heanue M, Colombet M, Boyle P. Estimates of the cancer incidence and mortality in Europe in 2006. *Ann Oncol* 2007; **18**: 581–592.
2. Ross JS, Schenkein DP, Pietrusko R, Rolfe M, Linette GP, Stec J *et al.* Targeted therapies for cancer 2004. *Am J Clin Pathol* 2004; **22**: 598–609.
3. Ashkenazi A. Targeting death and decoy receptors of the tumour-necrosis factor superfamily. *Nat Rev Cancer* 2002; **2**: 420–430.
4. Fesik SW. Promoting apoptosis as a strategy for cancer drug discovery. *Nat Rev Cancer* 2005; **5**: 876–885.
5. Ghobrial IM, Witzig TE, Adjei AA. Targeting apoptosis pathways in cancer therapy. *CA Cancer J Clin* 2005; **55**: 178–194.
6. Rowinsky EK. Targeted induction of apoptosis in cancer management: the emerging role of tumor necrosis factor-related apoptosis-inducing ligand receptor activating agents. *J Clin Oncol* 2005; **23**: 9394–9407.
7. Danial NN, Korsmeyer SJ. Cell death: critical control points. *Cell* 2004; **116**: 205–219.
8. Lowe SW, Cepero E, Evan G. Intrinsic tumour suppression. *Nature* 2004; **432**: 307–315.
9. Hanahan D, Weinberg RA. The hallmarks of cancer. *Cell* 2000; **100**: 57–70.
10. Thornberry NA, Lazebnik Y. Caspases: enemies within. *Science* 1998; **281**: 1312–1316.
11. Zimmermann KC, Bonzon C, Green DR. The machinery of programmed cell death. *Pharmacol Ther* 2001; **92**: 57–70.
12. Cory S, Adams JM. The Bcl2 family: regulators of the cellular life-or-death switch. *Nat Rev Cancer* 2002; **2**: 647–656.
13. Coultas L, Strasser A. The role of the Bcl-2 protein family in cancer. *Semin Cancer Biol* 2003; **13**: 115–123.
14. Willis SN, Fletcher JI, Kaufmann T, van Delft MF, Chen L, Czabotar PE *et al.* Apoptosis initiated when BH3 ligands engage multiple Bcl-2 homologs, not Bax or Bak. *Science* 2007; **315**: 856–859.
15. Salvesen GS, Duckett CS. IAP proteins: blocking the road to death's door. *Nat Rev Mol Cell Biol* 2002; **3**: 401–410.
16. Nagata S. Apoptosis by death factor. *Cell* 1997; **88**: 355–365.
17. Ashkenazi A, Dixit VM. Death receptors: signaling and modulation. *Science* 1998; **281**: 1305–1308.
18. Igney F, Krammer P. Death and anti-death: tumour resistance to apoptosis. *Nat Rev Cancer* 2002; **2**: 277–288.
19. LeBlanc HN, Ashkenazi A. Apo2L/TRAIL and its death and decoy receptors. *Cell Death Differ* 2003; **10**: 66–75.
20. Fulda S, Debatin KM. Extrinsic *versus* intrinsic apoptosis pathways in anticancer chemotherapy. *Oncogene* 2006; **25**: 4798–4811.
21. Ashkenazi A, Pai RC, Fong S, Leung S, Lawrence DA, Marsters SA *et al.* Safety and antitumor activity of recombinant soluble Apo2 ligand. *J Clin Invest* 1999; **104**: 155–162.
22. Walczak H, Miller RE, Ariail K, Gliniak B, Griffith TS, Kubin M *et al.* Tumoricidal activity of tumor necrosis factor-related apoptosis-inducing ligand *in vivo*. *Nat Med* 1999; **5**: 157–163.
23. Kelley S, Ashkenazi A. Targeting death receptors in cancer with Apo2L/TRAIL. *Curr Opin Pharmacol* 2004; **4**: 333–339.
24. Chuntharapai A, Dodge K, Grimmer K, Schroeder K, Marsters SA, Koeppen H *et al.* Isotype-dependent inhibition of tumor growth *in vivo* by monoclonal antibodies to death receptor 4. *J Immunol* 2001; **166**: 4891–4898.
25. Ichikawa K, Liu W, Zhao L, Wang Z, Liu D, Ohtsuka T *et al.* Tumoricidal activity of a novel anti-human DR5 monoclonal antibody without hepatocyte cytotoxicity. *Nat Med* 2001; **7**: 954–960.
26. Georgakis GV, Li Y, Humphreys R, Andreeff M, O'Brien S, Younes M *et al.* Activity of selective fully human agonistic antibodies to the TRAIL death receptors TRAIL-R1 and TRAIL-R2 in primary and cultured lymphoma cells: induction of apoptosis and enhancement of doxorubicin- and bortezomib-induced cell death. *Br J Haematol* 2005; **130**: 501–510.
27. Pukac L, Kanakaraj P, Humphreys R, Alderson R, Bloom M, Sung C *et al.* HGS-ETR1, a fully human TRAIL-receptor 1 monoclonal antibody, induces cell death in multiple tumour types *in vitro* and *in vivo*. *Br J Cancer* 2005; **92**: 1430–1441.
28. Guo Y, Chen C, Zheng Y, Zhang J, Tao X, Liu S *et al.* A novel anti-human DR5 monoclonal antibody with tumoricidal activity induces caspase-dependent and caspase-independent cell death. *J Biol Chem* 2005; **280**: 41940–41952.
29. Motoki K, Mori E, Matsumoto A, Thomas M, Tomura T, Humphreys R *et al.* Enhanced apoptosis and tumor regression induced by a direct agonist antibody to tumor necrosis factor-related apoptosis-inducing ligand receptor 2. *Clin Cancer Res* 2005; **11**: 3126–3135.
30. Tolcher AW, Mita M, Meropol NJ, von Mehren M, Patnaik A, Padavic K *et al.* Phase I pharmacokinetic and biologic correlative study of mapatumumab, a fully human monoclonal antibody with agonist activity to tumor necrosis factor-related apoptosis-inducing ligand receptor-1. *J Clin Oncol* 2007; **25**: 1390–1395.
31. Zhang L, Zhang X, Barrisford GW, Olumi AF. Lexatumumab (TRAIL-receptor 2 mAb) induces expression of DR5 and promotes apoptosis in primary and metastatic renal cell carcinoma in a mouse orthotopic model. *Cancer Lett* 2007; **251**: 146–157.
32. Plummer R, Attard G, Pacey S, Li L, Razak A, Perrett R *et al.* Phase 1 and pharmacokinetic study of lexatumumab in patients with advanced cancers. *Clin Cancer Res* 2007; **13**: 6187–6194.
33. Hymowitz S, Christinger H, Fuh G, Ultsch M, O'Connell M, Kelley R *et al.* Triggering cell death: the crystal structure of Apo2L/TRAIL in a complex with death receptor 5. *Mol Cell* 1999; **4**: 563–571.
34. Hymowitz S, O'Connell M, Ultsch M, Hurst A, Totpal K, Ashkenazi A *et al.* A unique zinc-binding site revealed by a high-resolution X-ray structure of homotrimeric Apo2L/TRAIL. *Biochemistry* 2000; **39**: 633–640.
35. Austin CD, Lawrence DA, Peden AA, Varfolomeev EE, Totpal K, De Maziere AM *et al.* Death-receptor activation halts clathrin-dependent endocytosis. *Proc Natl Acad Sci USA* 2006; **103**: 10283–10288.
36. Buchsbaum DJ, Zhou T, Lobuglio AF. TRAIL receptor-targeted therapy. *Future Oncol* 2006; **2**: 493–508.
37. Cha SS, Kim MS, Choi YH, Sung BJ, Shin NK, Shin HC *et al.* 2.8 Å resolution crystal structure of human TRAIL, a cytokine with selective antitumor activity. *Immunity* 1999; **11**: 253–261.
38. Mongkolsapaya J, Grimes J, Chen N, Xu X, Stuart D, Jones E *et al.* Structure of the TRAIL–DR5 complex reveals mechanisms conferring specificity in apoptotic initiation. *Nat Struct Biol* 1999; **6**: 1048–1053.
39. Lawrence D, Shahrokh Z, Marsters S, Achilles K, Shih D, Mounho B *et al.* Differential hepatocyte toxicity of recombinant Apo2L/TRAIL versions. *Nat Med* 2001; **7**: 383–385.
40. Ganten TM, Koschny R, Sykora J, Schulze-Bergkamen H, Buchler P, Haas TL *et al.* Preclinical differentiation between apparently safe and potentially hepatotoxic applications of TRAIL either alone or in combination with chemotherapeutic drugs. *Clin Cancer Res* 2006; **12**: 2640–2646.
41. Mori E, Thomas M, Motoki K, Nakazawa K, Tahara T, Tomizuka K *et al.* Human normal hepatocytes are susceptible to apoptosis signal mediated by both TRAIL-R1 and TRAIL-R2. *Cell Death Differ* 2004; **11**: 203–207.
42. Kelley RF, Totpal K, Lindstrom SH, Mathieu M, Billeci K, Deforge L *et al.* Receptor-selective mutants of apoptosis-inducing ligand 2/tumor necrosis factor-related apoptosis-inducing ligand reveal a greater contribution of death receptor (DR) 5 than DR4 to apoptosis signaling. *J Biol Chem* 2005; **280**: 2205–2212.
43. MacFarlane M, Kohlhaas SL, Sutcliffe MJ, Dyer MJ, Cohen GM. TRAIL receptor-selective mutants signal to apoptosis via TRAIL-R1 in primary lymphoid malignancies. *Cancer Res* 2005; **65**: 11265–11270.
44. Wagner KW, Punnoose EA, Januario T, Lawrence DA, Pitti RM, Lancaster K *et al.* Death-receptor O-glycosylation controls tumor-cell sensitivity to the proapoptotic ligand Apo2L/TRAIL. *Nat Med* 2007; **13**: 1070–1077.
45. Sheridan J, Marsters S, Pitti R, Gurney A, Skubatch M, Baldwin D *et al.* Control of TRAIL-induced apoptosis by a family of signaling and decoy receptors. *Science* 1997; **277**: 818–821.
46. Marsters S, Sheridan J, Pitti R, Huang A, Skubatch M, Baldwin D *et al.* A novel receptor for Apo2L/TRAIL contains a truncated death domain. *Curr Biol* 1997; **7**: 1003–1006.
47. Emery JG, McDonnell P, Burke MB, Deen KC, Lyn S, Silverman C *et al.* Osteoprotegerin is a receptor for the cytotoxic ligand TRAIL. *J Biol Chem* 1998; **273**: 14363–14367.
48. Kunkel TA, Roberts JD, Zakour RA. Rapid and efficient site-specific mutagenesis without phenotypic selection. *Methods Enzymol* 1987; **154**: 367–382.
49. Lee CV, Liang WC, Dennis MS, Eigenbrot C, Sidhu SS, Fuh G. High-affinity human antibodies from phage-displayed synthetic Fab libraries with a single framework scaffold. *J Mol Biol* 2004; **340**: 1073–1093.
50. Presta LG, Chen H, O'Connor SJ, Chisholm V, Meng YG, Krummen L *et al.* Humanization of an anti-vascular endothelial growth factor monoclonal antibody for the therapy of solid tumors and other disorders. *Cancer Res* 1997; **57**: 4593–4599.

Supplementary Information accompanies the paper on Cell Death and Differentiation website (http://www.nature.com/cdd)